Quantum entanglement and the dissociation process of diatomic molecules

2011 J. Phys. B: At. Mol. Opt. Phys. 44 175101

(http://iopscience.iop.org/0953-4075/44/17/175101)

J. Phys. B: At. Mol. Opt. Phys. **44** (2011) 175101 (13pp) doi:10.1088/0953-4075/44/17/175101

Quantum entanglement and the dissociation process of diatomic molecules

Rodolfo O Esquivel[1,2], Nelson Flores-Gallegos[3], Moyocoyani Molina-Espíritu[1], A R Plastino[2,4], Juan Carlos Angulo[2], Juan Antolín[5] and Jesús S Dehesa[2]

[1] Departamento de Química, Universidad Autónoma Metropolitana, 09340-México DF, Mexico
[2] Instituto Carlos I de Física Teórica y Computacional, and Departamento de Física Atómica, Molecular y Nuclear, Universidad de Granada, 18071-Granada, Spain
[3] Unidad Profesional Interdisciplinaria de Ingeniería, Campus Guanajuato del Instituto Politécnico Nacional, 36275-Guanajuato, Mexico
[4] National University La Plata, CREG-UNLP-Conicet, CC 727, 1900 La Plata, Argentina
[5] Departamento de Física Aplicada, EUITIZ, Universidad de Zaragoza, 50018-Zaragoza, Spain

E-mail: esquivel@xanum.uam.mx and arplastino@ugr.es

Received 1 June 2011, in final form 15 July 2011
Published 12 August 2011
Online at stacks.iop.org/JPhysB/44/175101

Abstract
In this work, we investigate quantum entanglement-related aspects of the dissociation process of some selected, representative homo- and heteronuclear diatomic molecules. This study is based upon high-quality *ab initio* calculations of the (correlated) molecular wavefunctions involved in the dissociation processes. The values of the electronic entanglement characterizing the system in the limit cases corresponding to (i) the united-atom representation and (ii) the asymptotic region when atoms dissociate are discussed in detail. It is also shown that the behaviour of the electronic entanglement as a function of the reaction coordinate R exhibits remarkable correspondences with the phenomenological description of the physically meaningful regimes comprising the processes under study. In particular, the extrema of the total energies and the electronic entanglement are shown to be associated with the main physical changes experienced by the molecular spatial electronic density, such as charge depletion and accumulation or bond cleavage regions. These structural changes are characterized by several selected descriptors of the density, such as the Laplacian of the electronic molecular distributions (LAP), the molecular electrostatic potential (MEP) and the atomic electric potentials fitted to the MEP.

(Some figures in this article are in colour only in the electronic version)

1. Introduction

Quantum entanglement constitutes one of the most fundamental and intriguing phenomena in nature. Current research on quantum entanglement is shedding new light on the basic properties of diverse many-body and few-body quantum systems [1–11]. In this vein, several researchers have investigated in recent years the phenomenon of entanglement in atomic physics [2–10]. A natural extension of these studies is to consider the entanglement-related aspects of molecular systems and chemical processes. In fact, there are several motivations for embarking on these lines of enquiry. Some of the most feasible proposals for the implementation of quantum computer technology, where entanglement plays a central role [12], are based upon quantum dots and quantum dot molecules (see [13–15] and references therein). These developments are clearly approaching the realms of molecular physics and quantum chemistry. There are other recent works suggesting that quantum entanglement may be highly relevant in scenarios involving chemical systems. It is worth mentioning in this regard exciting new ideas advanced in the emerging field of 'quantum biology' [16–18]. One sees that, as a general trend, several current lines of research related to the phenomenon of quantum entanglement are

entering a region where the spheres of interest of physics and chemistry overlap. It is thus natural for both physicists and chemists to explore systematically the implications of quantum entanglement for the study of chemical problems. Entanglement is almost universally present when one considers composite quantum systems constituted by interacting subsystems. In particular, entanglement usually shows up when a quantum system dissociates into its constituting parts. These are obviously some of the scenarios normally considered when dealing with chemical systems or processes. However, studies where the entanglement features of chemical systems are explicitly investigated by recourse to the evaluation of quantitative entanglement measures are scarce. For instance, there are recent studies concerning entanglement in the H_2 molecule [19] and in ethylene [20]. These developments are contained within the more general program of exploring the information-theoretical features exhibited by atomic and molecular systems [21–28].

In this study, we investigate the changes of the electronic entanglement (that is, the entanglement between the electrons in the system) during elementary dissociation processes of homonuclear (H_2, He_2, Li_2 and Cl_2) and heteronuclear (HCl) molecular systems. To this end we shall use correlated high-quality molecular wavefunctions calculated by recourse to state-of-the-art *ab initio* methods. To characterize the electronic entanglement of the system, we employ a quantitative measure of entanglement based on the von Neumann entropy of the (electronic) single-particle density matrix. Our aim is to investigate how the aforementioned entanglement evolution is correlated with the changes experienced by other relevant physical quantities characterizing the molecular system. In this regard, the total energy of the system plays a clear central role. In fact, the behaviour of the energy as a function of the molecular interatomic distance R (the 'reaction coordinate') contains important information about the basic features of the dissociation process. Two limit cases can be identified in a plot of the energy against the interatomic distance: a united-atom representation corresponding to the limit of vanishing distance and, in the limit of large interatomic distances, a dissociated system. We shall see that the transition between these two configurations manifests itself both in the behaviour of the energy and in the behaviour of the electronic entanglement. However, the information about the dissociation process yielded by these two quantities is not equivalent. It will be shown in this study that the electronic entanglement is able to reveal all of the critical points exhibited by the electronic density during the dissociation process, such as accumulation and depletion of charge and bond breaking. In contrast, most of these structural changes have no observable counterpart in the energy profile. To analyse these structural modifications in the spatial electronic distribution we are going to use appropriate descriptors, such as the Laplacian of the electron spatial density, the molecular electrostatic potential (MEP) and the electric atomic potentials. The usefulness of these descriptors has been assessed in recent studies by some of the authors of this work [29].

2. Electronic entanglement and descriptors of the electronic spatial distribution

As already mentioned, our present aim is to investigate the relationships between the evolution of the electronic entanglement during the dissociation process, on the one hand, and the main structural changes of the system occurring as this process takes place, on the other one. Appropriate descriptors of the electronic density are used in order to visualize these changes. In this section, we provide a brief review of the basic ideas concerning entanglement between identical fermions, which we are going to need in order to evaluate the electronic entanglement. We also explain briefly the descriptors of the chemical structural changes that we shall use in this study. All physical quantities are expressed in atomic units (au) except distances, which are given in armstrongs.

2.1. Entanglement between identical fermions

Quantum entanglement in systems consisting of N identical fermions has been the focus of several research efforts in recent years [1, 30–37]. Entanglement between fermions has been investigated in connection with a variety of systems. For instance, research has been devoted to study entanglement in two-electron atomic models [3] and entanglement between pairs of electrons in conducting bands [33], among many others.

A pure state of a system constituted by N identical fermions is non-entangled (that is, separable) if it is expressible as a single Slater determinant $\det\{|1\rangle, |2\rangle, \ldots, |N\rangle\}$ constructed with N normalized and orthogonal single-particle states $\{|i\rangle, i = 1, \ldots, N\}$. N-fermion states that admit this representation are said to have Slater rank equal to 1. Pure states of N identical fermions that cannot be cast in the alluded way are entangled. Note that the minimum correlations between the particles required by the antisymmetry of the fermionic state do not contribute to the state's entanglement. In other words, the fermionic entanglement of an N-fermion state is given by the quantum correlations that the state has on top of these minimum ones. There are deep physical reasons for adopting this notion of fermionic entanglement (see [1, 30, 31]).

Let $|\Psi\rangle$ denote a pure state of N identical fermions. The single-particle reduced density matrix, obtained by taking the trace over $N-1$ particles, is then $\rho_r = \mathrm{Tr}_{2,3,\ldots,N}(|\Psi\rangle\langle\Psi|)$. The von Neumann entropy of ρ_r, given by $S(\rho_r) = -\mathrm{Tr}(\rho_r \ln \rho_r)$, leads to a natural quantitative measure for the amount of entanglement of the state $|\Psi\rangle$,

$$\xi_{vN}[|\Psi\rangle] = S(\rho_r) - \ln N. \tag{1}$$

The entanglement measure (1) constitutes a non-negative quantity that vanishes if and only if the state $|\Psi\rangle$ has the Slater rank 1 and is therefore non-entangled. The term $-\ln N$ appearing in (1) takes into account the fact that even in the separable case (represented by a Slater determinant) the entropy of the reduced single-particle density matrix does not vanish and is equal to $\ln N$. In the particular case $N = 2$, the measure (1) can be related to the Schmidt decomposition of pure states of two identical fermions. The measure (1) (or a

similar one defined in terms of the linear entropy) has been applied to several problems, particularly in connection with two-fermion systems (for a recent discussion on the theoretical foundations of the measure (1) see [37]).

Eigenfunctions of the first-order reduced density matrix ρ_r are usually called natural spin orbitals after Löwdin [38] and their corresponding eigenvalues are the natural spin occupation numbers $\{n_i^\gamma; i = 1, \ldots, \mathcal{M}\}$, with $\mathcal{M}$ standing for the number of orbitals and γ for the α or β spin majority channels. Natural spin orbitals are obtained by performing symmetric (orthogonal) transformations on the density matrix so as to obtain its diagonal form characterized by a spectral decomposition representing the symmetry point group of the molecule (unless an atomic partitioning scheme is employed [39, 40]). The first-order reduced density matrix is normalized to 1, $\mathrm{Tr}(\rho_r) = 1$.

The aim of this work is to calculate the von Neumann entropy $S(\rho_r) = -\mathrm{Tr}(\rho_r \ln \rho_r)$ of the electronic single-particle reduced density matrix ρ_r of several diatomic molecules in order to analyse their (electronic) entanglement features as a function of the interatomic distance R. To evaluate $S(\rho_r)$ we shall use Löwdin's spectral decomposition of the matrix ρ_r, leading to

$$S(\rho_r) = -\sum_{i,\gamma} n_i^\gamma \ln n_i^\gamma . \tag{2}$$

From $S(\rho_r)$ the entanglement measure given by equation (1) can be obtained straightforwardly. It is worth mentioning that closed-shell molecular and atomic systems are commonly represented through a 'double occupied' reduced density matrix $\rho_r^{(\mathrm{DO})}$ with eigenvalues $\left(n_i^\alpha + n_i^\beta\right)$ such that $\sum_i (n_i^\alpha + n_i^\beta) = 1$. Therefore, ξ_{vN} can be expressed in an equivalent manner as $\xi_{vN} = S\left[\rho_r^{(\mathrm{DO})}\right] - \ln \frac{N}{2}$, where $S\left[\rho_r^{(\mathrm{DO})}\right] = -\sum_i \left(n_i^\alpha + n_i^\beta\right) \ln \left(n_i^\alpha + n_i^\beta\right)$ is the von Neumann entropy corresponding to the double-occupation density matrix $\rho_r^{(\mathrm{DO})}$.

2.2. *Descriptors of the electronic spatial density*

In order to characterize the stationary points of the energy profile as well as other features of the system, several descriptors of the electronic distributions are employed: the Laplacian of the electron density, the MEP and the atomic electric potentials (EP). Regions of charge accumulation and depletion are analysed by recourse to contours of the isosurface of the Laplacian of the density (LAP). Similarly, the nucleophilic/electrophilic regions are described through contours of the isosurface of the MEP.

The Laplacian of the electron density (LAP), $\nabla^2\rho$, provides interesting information about the chemical bonding [41]. In regions where the Laplacian is negative the electronic charge is accumulated (this is represented in contour diagrams of blue-coloured shades). On the other hand, in regions where the Laplacian is positive a depletion of electronic charge occurs (which is represented in contour diagrams of red-coloured shades). Consequently, the LAP constitutes a useful tool for the study of two basic aspects of a chemical process: the charge concentration in the valence shell of the base (nucleophile) and the charge depletion in the valence shell of the acid (electrophile).

The MEP represents the electrostatic potential energy of a proton at a particular location within a molecule [42], say at the location of the nucleus A. Then, the electrostatic potential, V_A, is defined as

$$V_A = \sum_{B \neq A} \frac{Z_B}{|\vec{R}_B - \vec{R}_A|} - \int \frac{\rho(\vec{r})\, \mathrm{d}\vec{r}}{|\vec{r} - \vec{R}_A|}, \tag{3}$$

where $\rho(\vec{r})$ is the molecular electron density and Z_B is the charge on nucleus B, located at $\vec{R}_B$. Generally speaking, negative electrostatic potential corresponds to an attraction of the proton by the concentrated electron density in the molecules from lone pairs, pi-bonds, etc (in contour diagrams of red-coloured shades). Positive electrostatic potential corresponds to a repulsion of the proton by the atomic nuclei in regions where low electron density exists and the nuclear charge is incompletely shielded (in contour diagrams of blue-coloured shades). The most popular methods for extracting charges from molecular wavefunctions are based on fitting of the atomic charges to the MEP computed with *ab initio* methods. The charge fitting procedure consists of minimizing the root-mean squared deviation between the Coulombic potential generated by the atomic charges and the MEP. The nonbonded EP (atomic) will be employed throughout the study since they provide useful information about the atomic extent capacity for acquiring charge.

3. Entanglement and the dissociation of diatomic molecules

This study is performed by tracking the dissociation path of homonuclear and heteronuclear diatomic molecules: H_2, $He\cdots He$, Li_2, Cl_2 and HCl. Löwdin's natural orbital-based representation of the electronic single-particle reduced density matrix, necessary for the von Neumann entropy and electronic entanglement calculations, was obtained by use of *ab initio* calculations of high-quality correlated molecular wavefunctions determined according to *QCISD* and *CCSD*. These wavefunctions were obtained by recourse to different choices of basis sets, either Pople [43]: *6-31G*, *6-311G*, *6-311++G(d,p)* or Dunning [44]: *cc-pVTZ* and *cc-pVQZ*. Physically, these numerical procedures correspond to state-of-the-art, post-Hartree–Fock computational methods of a variational nature, as opposed to other strategies which employ perturbative approaches. This choice ensures the proper energy convergence for the calculations. Besides, the above-mentioned basis sets employed to span the wavefunctions are known to provide an adequate representation of the molecular wavefunctions in the physically relevant domain of the corresponding electron densities. The electronic structure calculations were carried out with the *Gaussian 03* suite of programs [45]. It is worth mentioning that all reported values shown in tables 1 and 2 and depicted in figures 1 through 20 were obtained at the highest levels of theory performed in this study, i.e. at the *QCISD* and *CCSD* ones and with Dunning basis sets. Regions of accumulation/depletion of the electronic distributions were analysed using the contours of the isosurfaces of the Laplacian of the density (LAP). The contours of the isosurfaces of the MEP were employed to analyse the

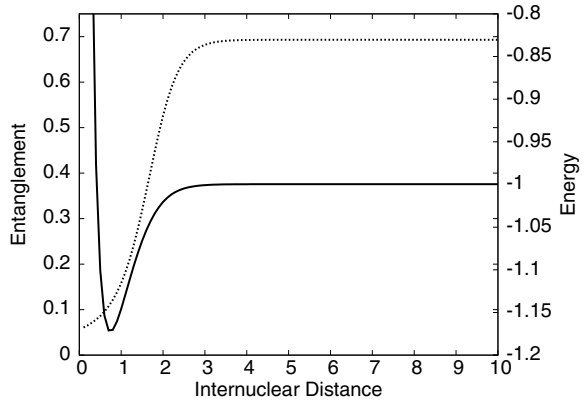

Figure 1. Entanglement (dotted line) and total energy (solid line) for the dissociation process of the hydrogen molecule.

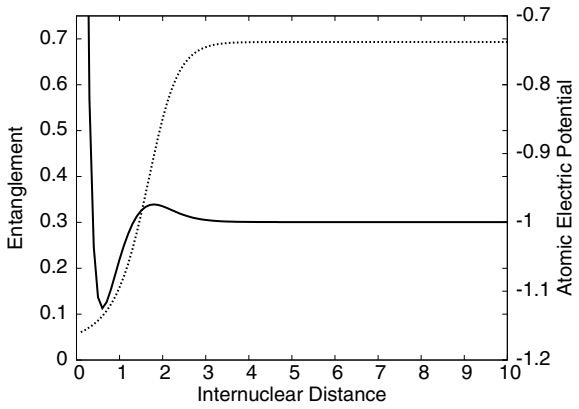

Figure 2. Entanglement (dotted line) and the atomic EP (solid line) for the dissociation process of the hydrogen molecule.

Table 1. von Neumann entropy (equation (2)) and the entanglement measure (equation (1)) of the molecular system in the limit $R \to 0$. The entropy of the corresponding 'united atom' is also given for comparison.

Molecular system			United atom	
Molecule	vN-entropy	ξ_{vN}	Atom (state[a])	vN-entropy
H_2	0.753	0.060	He (S)	0.751
He···He	1.586	0.199	Be (S)	1.595
Li_2	1.894	0.102	C (T)	1.890
Cl_2	3.565	0.038	Se (D)	3.554
HCl	2.940	0.049	Ar (S)	2.942

[a] Notation stands for S-singlet state, T-triplet state, etc.

nucleophilic/electrohilic regions (negative/positive MEP). The two aforementioned scalar functions were calculated by the use of MOLDEN [46]. The atomic EP fitted to the MEP were obtained with the CHELPG method [45, 47].

With the aim of analysing the behaviours of the von Neumann entropy $S(\rho_r)$ and the electronic entanglement ξ_{vN} during the course of the molecular dissociation, we have tabulated the values adopted by these two quantities, jointly with the values of the molecular and atomic energies, at two limit regimes: at the united-atom representation when $R \to 0$ (table 1) and at the asymptotic limit as $R \to \infty$ (table 2). Both cases are illuminating in order to achieve a complete perspective of the physical phenomena occurring at all stages of the dissociation on the light of the electronic *entanglement* of the molecular system. The particular characteristics for each molecular case will be discussed separately.

3.1. Hydrogen molecule

The electronic entanglement (1) corresponding to the H_2 molecule, together with the total energy and the atomic EP, respectively, is depicted in figures 1 and 2 against the interatomic distance R. We can observe in these figures that at the dissociation stage ($R > 2$ Å) the system's electronic entanglement shows a profile similar to the one exhibited by the energy. Of particular interest are the specific features of these physical quantities at the united-atom region ($R \to 0$), which in this case corresponds to a helium-like atom and, also, at the asymptotic region ($R \to \infty$) where the two hydrogenic atoms lose their Coulombic interactions (bonding). The analysis of these cases allows us to indagate into the nature of the quantum correlations (entanglement). Thus, in table 1 we observe, in the limit $R \to 0$, close agreement between the entropy $S(\rho_r)$ associated with the molecule and the value of this quantity corresponding to a helium united-atom representation in its stable configuration (singlet state). It is worth mentioning that this agreement constitutes cogent evidence for the quality of the present results, even in the vicinity of the computationally problematic $R = 0$ singularity. As the internuclear distance increases, $S(\rho_r)$ grows, eventually reaching a constant value at the dissociation region. In this limit regime, the H_2 molecule dissociates and the entropy of the system's electronic single-particle reduced density matrix ρ_r tends to the value $2 \ln 2$ (see table 2). Therefore, we see that even for large values of the reaction coordinate R the system still exhibits a finite amount of (electronic) entanglement. Note from table 2 that the energy of the system for large R is almost twice the atomic energy of each hydrogenic atom. The asymptotic behaviour of the electronic entanglement of the H_2 molecule can be understood physically if we consider an (approximate) representation of the wavefunction in terms of hydrogen atomic orbitals. In the limit of large values of the distance between the two protons ($R \to \infty$), the electronic wavefunction of the system tends to

$$\frac{1}{\sqrt{2}}[\Psi_{100}(\vec{r}_1 - \vec{R}_a)\Psi_{100}(\vec{r}_2 - \vec{R}_b) + \Psi_{100}(\vec{r}_1 - \vec{R}_b)\Psi_{100}(\vec{r}_2 - \vec{R}_a)]\,\chi_{12}, \tag{4}$$

where $\vec{R}_{a,b}$ are the position vectors of the two protons, $\vec{r}_{1,2}$ are the position vectors of the two electrons, $\Psi_{nlm}(\vec{r})$ denote the standard hydrogenic eigenfunctions and $\chi_{12} = \frac{1}{\sqrt{2}}(|+-\rangle - |-+\rangle)$ is the singlet spin wavefunction. The distance between the two protons is $R = |\vec{R}_a - \vec{R}_b|$. Note that when $R \to \infty$ the overlap between the spatial wavefunctions $\Psi_{100}(\vec{r} - \vec{R}_a)$ and $\Psi_{100}(\vec{r} - \vec{R}_b)$ tends to zero. The wavefunction (4) cannot be expressed as a single Slater determinant. It describes two entangled electrons with $\xi_{vN} = \ln 2$. At least two Slater determinants are needed to express the state (4).

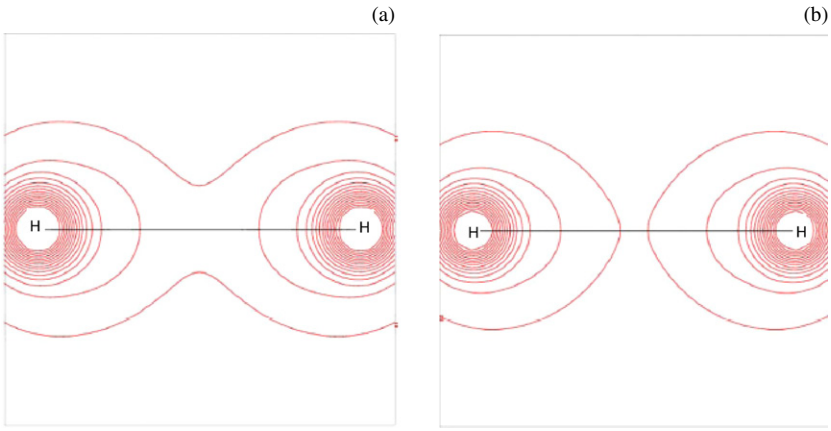

Figure 3. Contours of the isosurface of the LAP for the dissociation process of the hydrogen molecule at an internuclear distance of 0.72 Å (left) and 0.76 Å (right).

Table 2. von Neumann entropy (equation (2)), entanglement (equation (1)) and energy of the molecular system in the limit $R \to \infty$. The corresponding quantities associated with the atoms resulting from the dissociation process are also given for comparison.

	Energy		von Neumann entropy					
System	Molecule	Atom[a]	Molecule	Atom (S)	Atom (D)	Atom (T)	Tendency	ξ_{vN}
H_2	−1.000	−1	1.386	–	0	–	$2\ln 2$	0.693
He···He	−5.805	−5.805	1.445	0.751	–	0.697	1.444[b]	0.058
Li_2	−14.865	−14.865	2.024[c]	–	1.330	–	1.330 (Li)[d]	0.231
Cl_2	−919.281	−919.372	3.610[c]	–	2.887	–	2.887 (Cl)[d]	0.083
HCl	−460.117	−460.186	2.996	2.953	–	–	2.953 (Cl^-)[e]	0.105

[a] Sum of the energies of the individual atoms at the dissociation limit ($R \to \infty$).
[b] Entropy sum of the dissociated atomic states of helium.
[c] The molecular entropy value constrained to the double occupation of ρ_r agrees fairly well with the reported atomic value in the table, see the text.
[d] Entropy of the dissociated atomic state of highest multiplicity.
[e] Entropy of the dissociated atomic state for the anion of chlorine.

Indeed, this state can be explicitly written as

$$\begin{aligned}&\tfrac{1}{\sqrt{2}}\big[\tfrac{1}{\sqrt{2}}(\Psi_{100}(\vec{r}_1-\vec{R}_a)\Psi_{100}(\vec{r}_2-\vec{R}_b)|+-\rangle\\&\quad-\Psi_{100}(\vec{r}_1-\vec{R}_b)\Psi_{100}(\vec{r}_2-\vec{R}_a)|-+\rangle)\\&\quad-\tfrac{1}{\sqrt{2}}(\Psi_{100}(\vec{r}_1-\vec{R}_a)\Psi_{100}(\vec{r}_2-\vec{R}_b)|-+\rangle\\&\quad-\Psi_{100}(\vec{r}_1-\vec{R}_b)\Psi_{100}(\vec{r}_2-\vec{R}_a)|+-\rangle)\big].\end{aligned}\tag{5}$$

In the limit $R \to \infty$, the system can be effectively regarded as comprising two independent, non-interacting hydrogen atoms. In that limit situation, the system admits the following pair of non-entangled eigenstates (each described by a single Slater determinant) sharing the same (two-fold) degenerate energy eigenvalue,

$$\begin{aligned}&\tfrac{1}{\sqrt{2}}(\Psi_{100}(\vec{r}_1-\vec{R}_a)\Psi_{100}(\vec{r}_2-\vec{R}_b)|+-\rangle\\&\quad-\Psi_{100}(\vec{r}_1-\vec{R}_b)\Psi_{100}(\vec{r}_2-\vec{R}_a)|-+\rangle)\\&\tfrac{1}{\sqrt{2}}(\Psi_{100}(\vec{r}_1-\vec{R}_a)\Psi_{100}(\vec{r}_2-\vec{R}_b)|-+\rangle\\&\quad-\Psi_{100}(\vec{r}_1-\vec{R}_b)\Psi_{100}(\vec{r}_2-\vec{R}_a)|+-\rangle).\end{aligned}\tag{6}$$

For large (but finite) values of R, the interaction between the two hydrogen atoms lifts the above degeneracy and leads to the entangled ground state (5). No matter how small the interaction is (that is, no matter how large R is), the degeneracy is going to be lifted and one will have the ground state (5) having a finite amount of entanglement. This state of affairs is similar to the one observed in two-electron atomic models, where some atomic eigenstates exhibit a considerable amount of entanglement even for an arbitrarily weak interaction between the electrons [9, 10]. An important feature of the state (4)–(5) is that, due to the fact that it involves the two spatially localized (that is, non-overlapping) wavefunctions $\Psi_{100}(\vec{r}-\vec{R}_a)$ and $\Psi_{100}(\vec{r}-\vec{R}_b)$, the spin degrees of freedom admit an effective description as two distinguishable qubits. That is, they behave as if they were two distinguishable qubits in the maximally entangled EPR (Einstein–Podolsky–Rosen) state $\frac{1}{\sqrt{2}}(|01\rangle - |10\rangle)$ [12].

More information about the dissociation process is shown in figures 3 and 4. These figures depict, respectively, the contours of the isosurfaces of the LAP and the MEP for values of R corresponding to the stationary points of the quantities shown in figures 1 and 2. Let us recall that the LAP is useful to unveil regions of charge 'concentration/depletion' whereas the MEP is helpful to analyse regions of low negative charge (positive potential) or negative charge accumulation (negative potential), i.e. electrophilic or nucleophilic regions, respectively. Along these lines, figure 3 permits the

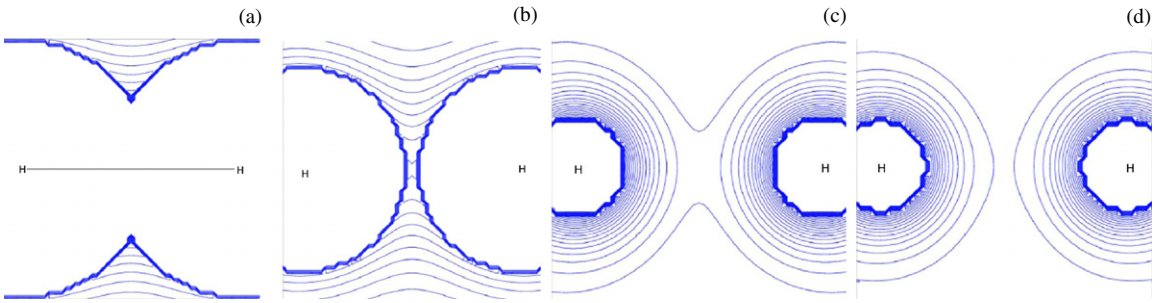

Figure 4. Contours of the isosurface of the MEP for the dissociation process of the hydrogen molecule at an internuclear distance of 0.78 Å (left), 1.0 Å, 2.2 Å and 2.5 Å (right).

identification of a point around 0.7 Å where the charge depletion at the bonding region gets completed and the equilibrium internuclear distance is reached (see figure 1), indicating a bond forming situation. Note that this point is also detected by the atomic EP for the hydrogenic species, showing a minimum extent capacity to acquire more electronic charge, which was developing prior to reaching this region (see figure 2). This feature also indicates a bond forming situation. The interesting observation is that the electronic entanglement of the molecule starts growing rapidly beyond this point. On the other hand, figure 4 shows several interesting features detected by the MEP. At the vicinity of the equilibrium region (0.8 Å) the bond breaking starts, as revealed by the low density contours (see figure 4(a)) that enclose the atoms at 1.0 Å (see figure 4(b)). Remarkably, this coincides with an inflection point in the entanglement and with the increase of the total energy (see figure 1). Then, the EP shows a local maximum indicating that the hydrogenic atoms are getting their maximum capacity to acquire charge (at 1.9 Å, see figure 2) because of the bond cleavage situation which is shown at the onset of the dissociation region around 2.5 Å. The positive contours of the MEP (low density profiles in figures 4(c) and (d)) mark the end of the dissociation process. Beyond this region the EP gets constant as well as the total energy and the entanglement of the dissociated system (see figures 1 and 2).

3.2. Helium excimer

The diatomic molecular case of helium is known to form an excimer (excited dimer) [48], i.e. a short-lived dimeric system formed by two He atoms with (at least) one of them in an electronic excited state. It has been formed experimentally by high-pressure microhollow cathode discharge plasmas [49]. We have considered with special attention this particular system because it does not form a stable molecule and it represents an interesting test case for an entanglement analysis. In this manner, we proceed as in the hydrogen case, so that in figures 5 and 6 we have depicted the entanglement measure (equation (1)) along with the total energy and the atomic EP, respectively. It can be observed from the figures that as $R \to 0$ the entanglement measure corresponding to the excimer system possesses a finite value which fairly agrees with the united-atom representation for beryllium in its singlet state (see table 1). As expected, when the internuclear distance

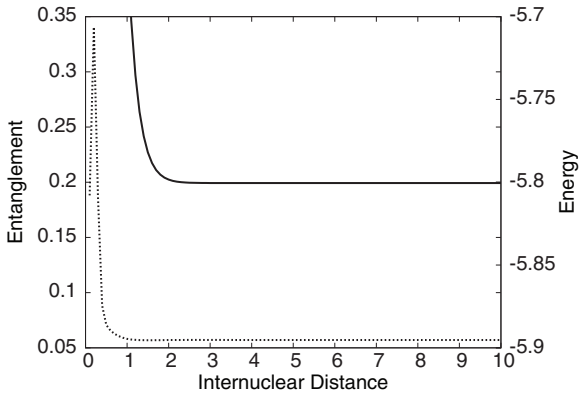

Figure 5. Entanglement (dotted line) and total energy (solid line) for the dissociation process of the excimer of helium.

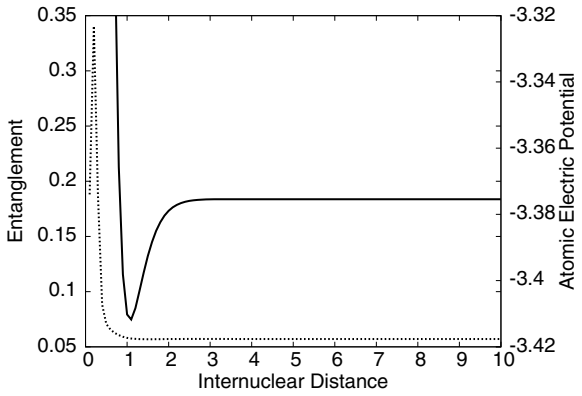

Figure 6. Entanglement (dotted line) and the atomic EP (solid line) for the dissociation process of the helium excimer.

increases the molecular system never becomes stable. This can be appreciated in the behaviour of the total energy depicted in figure 5. However, the entanglement measure indicates a quantum correlated system with a very small entanglement value of around 0.06 (see table 2). Note that, as happens in the case of hydrogen, the total energy of the system at large distances coincides with the sum of the atomic energies of a pair of helium atoms.

It will prove convenient to introduce the following notation. We shall denote by

$$\left|\Psi_{\beta_1}^{(\alpha_1)} \ldots \Psi_{\beta_N}^{(\alpha_N)}\right| \tag{7}$$

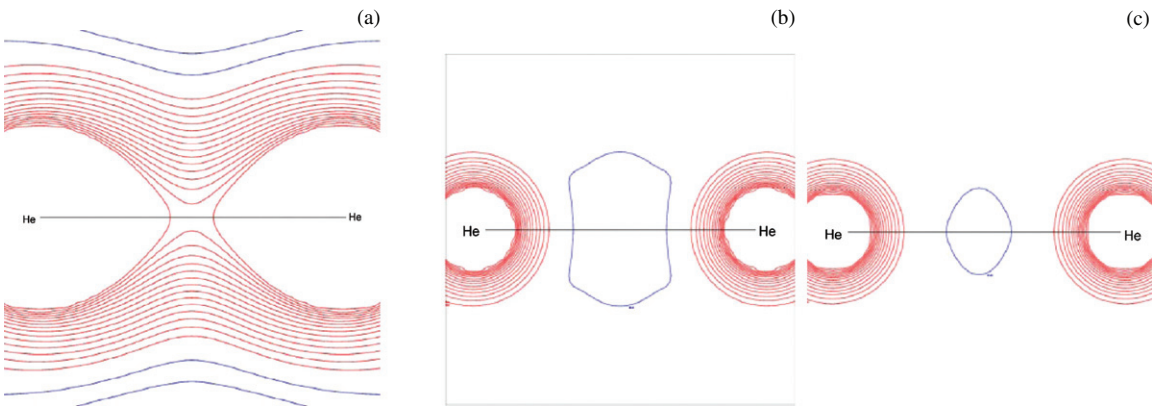

Figure 7. Contours of the isosurface of the LAP for the dissociation process of the helium excimer at an internuclear distance of 0.5 Å (left), 1.0 Å (center) and 1.05 Å (right).

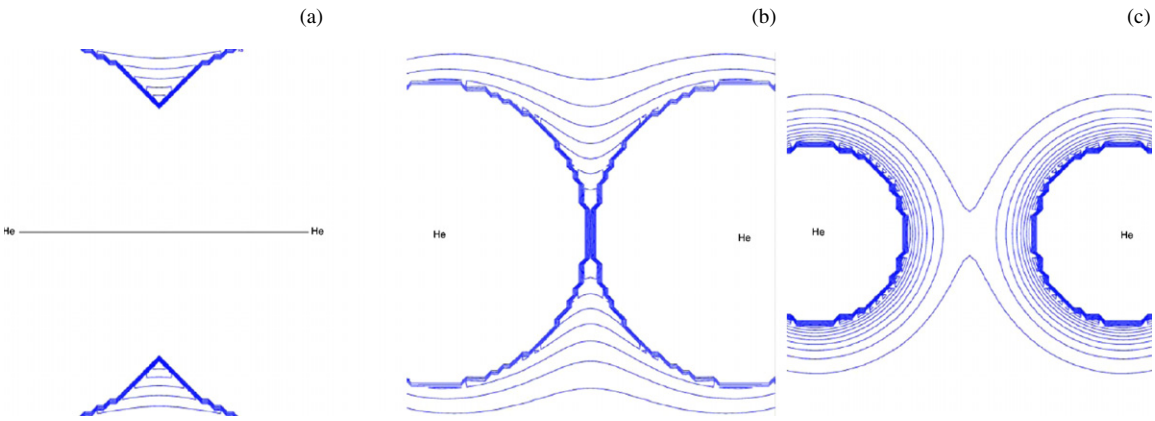

Figure 8. Contours of the isosurface of the MEP for the dissociation process of the helium excimer at an internuclear distance of 1.2 Å (left), 1.6 Å (center) and 2.6 Å (right).

the Slater determinant constructed with the N single-particle (normalized and orthogonal) wavefunctions

$$\Psi_{\beta_i}^{(\alpha_i)}(\vec{r}) = \Psi_{\beta_i}(\vec{r} - \vec{R}_{\alpha_i}), \tag{8}$$

where the labels α_i are equal to either a or b, the labels β_i correspond to any other parameters (quantum numbers) needed to characterize the above wavefunctions, $\vec{r}$ indicates the position of the electron and $\vec{R}_{a,b}$ the locations of the two nuclei. The labels β_i may, for instance, correspond to different combinations of the quantum numbers $nlm\pm$ associated with hydrogenic wavefunctions (the $\pm$ indices corresponding to the eigenvalues of the z component of the spin angular momentum). According to this notation, for example, the hydrogenic wavefunctions are denoted by

$$\Psi(\vec{r})_{nlm\pm}^{(a,b)} = \Psi_{nlm}(\vec{r} - \vec{R}_{a,b})\,|\pm\rangle, \tag{9}$$

where $|\pm\rangle$ are the eigenvectors of the z component of the spin angular momentum operator.

It is well known that the ground state of helium admits a reasonably good Hartree–Fock representation. In other words, the ground state of helium can be approximated relatively well by a Slater determinant $|\Psi_{\beta_1}\Psi_{\beta_2}|$. The low value of the electronic measure of entanglement corresponding to large values of the reaction coordinate R indicates that in this case the wavefunction of the molecular system also admits a good representation within the Hartree–Fock approximation. Indeed, the wavefunction is approximately given by the Slater determinant $\left|\Psi_{\beta_1}^{(a)}\Psi_{\beta_2}^{(b)}\Psi_{\beta_1}^{(b)}\Psi_{\beta_2}^{(a)}\right|$, where the single-particle wavefunctions Ψ_{β_1} and Ψ_{β_2} are those involved in the Hartree–Fock approximation for the ground state of helium.

The phenomenological behaviour of the excimer helium system might be unveiled through the stationary points of the quantities shown in figures 5 and 6 by use of the contours of the isosurface of the LAP and the MEP which are depicted in figures 7 and 8, respectively. First, note that the entanglement measure exhibits a very pronounced peak at 0.5 Å which clearly corresponds with the onset of the charge developing at the internuclear distance, as witnessed by the LAP with a reduction of charge depletion (in red-coloured shades in figure 7(a)) and the appearance of charge accumulation (in blue-coloured shades in figure 7(a)) at the bonding region. The end of the process is marked by a sudden change of the entanglement which becomes roughly constant at 1.0 Å. This is also indicated in the LAP contours (figures 7(b) and (c)), where it is revealed that bond charge never develops. That is why the system is unstable. It is worthy to note that the atomic EP indicates clearly the charge accumulation process at 1.0 Å since the minimum marks a point of least capacity for these atoms to gain charge. Indeed, charge is rapidly removed from the

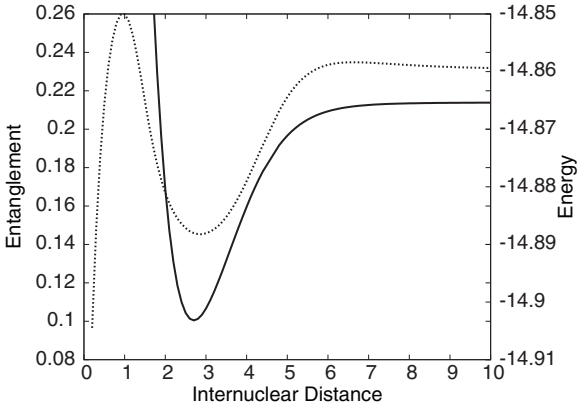

Figure 9. Entanglement (dotted line) and total energy (solid line) for the dissociation process of the lithium molecule.

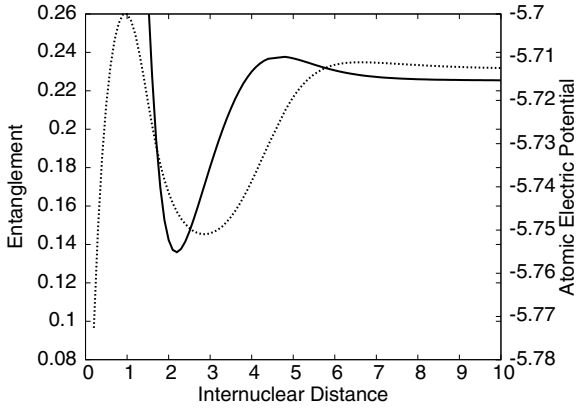

Figure 10. Entanglement (dotted line) and atomic EP (solid line) for the dissociation process of the lithium molecule.

internuclear region and concentrated in the vicinity of each atom. Beyond this region, the EP increases so as to reach a constant value. This observation is in agreement with the behaviour of the total energy (figure 5) which decays up to a constant value as the EP does. The interesting observation so far is that entanglement increases when accumulation of charge develops. Furthermore, the critical points of the quantities shown in figures 5 and 6 might also be analysed through the MEP. In figures 8(a)–(c), one can observe the process of molecular separation into atoms by developing an internuclear region of lower density at 1.2 Å. Here, the repulsive Coulombic interactions decrease although no charge remains so as to form a bond. This is witnessed by the total energy in figure 5 which decreases rapidly from 1.2 Å up to 1.6 Å where the MEP shows the atomic separation (figure 8(b)). Finally, as R increases no charge accumulation develops and the bond is lost (figure 8(c)). It is interesting to note that through this unstable system it is possible to witness the artificial formation of charge bonding, which has been analysed in other systems (stable) in the context of non-nuclear attractors or pseudoatoms [50, 51]. In our case, the entanglement measure as well as the EP indicates an artificial developing of charge at 1.0 Å as it is shown in the LAP diagrams (figures 7(b) and (c)).

3.3. Lithium molecule

Proceeding with the analysis for lithium molecule, we have depicted in figures 9 and 10 the entanglement measure (equation (1)) along with the total energy and the atomic EP, respectively. It can be observed from the figures that the entanglement measure as $R \to 0$ agrees well with the united-atom representation of carbon in its triplet state with a finite value for the entanglement measure (see table 1). On the other hand, by enlarging the internuclear distance beyond its equilibrium position the lithium dissociation is reached as $R \to \infty$ and the von Neumann entropy of the electronic single-particle reduced density matrix (when expressed in the double-occupation representation) approaches remarkably well the entropy for the atomic case in its stable D-state (see table 2). Note from table 2 that the total energy of the system coincides with the sum of the atomic energies.

The phenomenological description of Li_2 might be analysed through figures 9 to 12, where the contours of the isosurface of the LAP and the MEP are plotted (figures 11 and 12, respectively). For instance, the LAP shows a region where the charge is developing (charge accumulation in blue-coloured shades in figure 11(a)) and this is clearly indicated by the entanglement measure at 1.0 Å (see figures 9 and 10). Then, as the distance enlarges the accumulation process ends (see figure 11(b)) and this is marked by the decrease of the total energy (see figure 9). Moreover, the electrophilic/nucleophilic regions of the molecule are appreciated through the MEP which shows (see figure 12(a)) that at 0.1 Å the electrophilic behaviour enclosing the atoms indicates the ending of the accumulation charge process and hence the equilibrium situation is reached, what is revealed by the minimum of the total energy (figure 9) and anticipated by the atomic EP at 2.1 Å (figure 10) where the atoms reached their minimum capacity to acquire more charge; thus, electrostatic stability is reached. It is interesting to note that the minimum of the entanglement measure occurs at the same point as that one of the total energy, indicating that the behaviour of the electronic entanglement reveals the location of the equilibrium configuration.

The lithium molecule possesses an additional interesting feature which is the evidence of non-nuclear maxima [50, 51] that may vary by shortening or enlarging the internuclear distance. For instance, it has been reported that a non-nuclear maximum appears when the bond length is increased [52]. Through the MEP analysis we have been able to unveil the formation of such a non-nuclear attractor beyond the equilibrium distance, i.e. at 3.6 Å we observe from figure 12(b) the formation of concentration of charge (depicted in red-coloured shades) which coincides quite well with the distance reported in the literature [50, 52]. At larger distances the atoms dissociate and this is indicated by the electrophilic regions of the MEP in figure 12(c) where all quantities become roughly constant.

3.4. Chlorine molecule

The analysis for the chlorine molecule proceeds in an analogous manner as it has been previously discussed. In

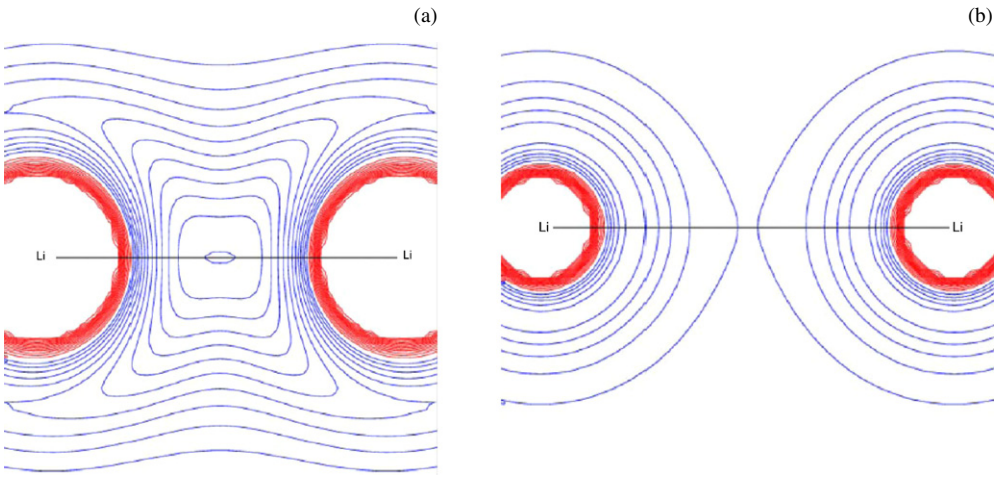

Figure 11. Contours of the isosurface of the LAP for the dissociation process of the lithium molecule at an internuclear distance of 0.9 Å (left) and 1.4 Å (right).

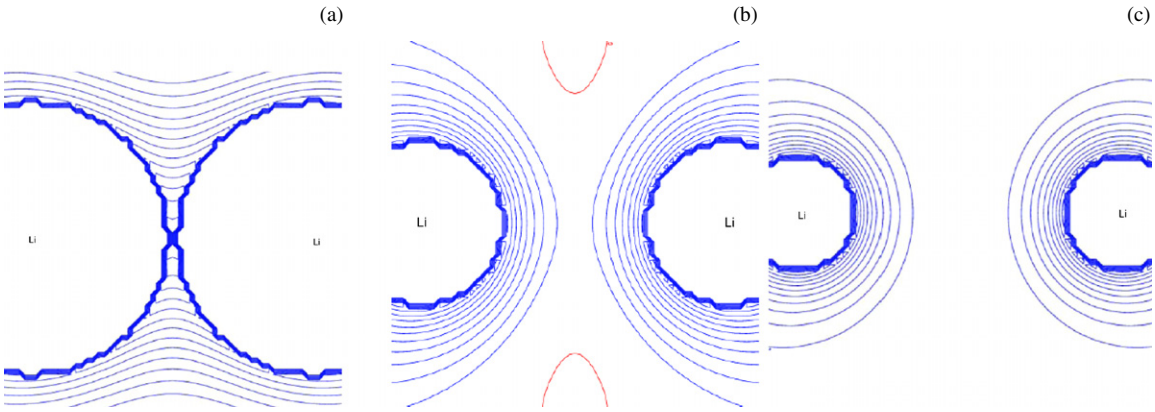

Figure 12. Contours of the isosurface of the MEP for the dissociation process of the lithium molecule at an internuclear distance of 2.1 Å (left), 3.6 Å (center) and 5.5 Å (right).

figures 13 and 14, we show the values for the entanglement measure (equation (1)) along with the total energy and the atomic EP, respectively. In table 1, we observe that in the limit $R \rightarrow 0$ (united atom) there is good agreement between the von Neumann entropy of the electronic, single-particle density matrix associated with the molecular system, on the one hand, and that one associated with the selenium atom (which possesses a doublet spin state) on the other one. At the other end, in the dissociation region $R \rightarrow \infty$, the von Neumann entropy of ρ_r (when expressed in the double-occupation representation) approaches a limit value that corresponds to that of the chlorine atomic system in its state of maximum multiplicity (D-state, see table 2). Note that at this point the total energy of the system becomes twice the atomic energy of the chlorine atom (table 2).

The physical description of the process might be followed by the isosurface of the LAP (figure 15) and the MEP (figure 16). For instance, at 0.8 Å the density of the molecular system gets lumped together and it may be noticed from figure 15(a) that more external shells of the atoms are forming. This is interesting and the event is indicated by the maximum of entanglement measure at this point as it may be observed from figure 13. Then, at 1.2 Å the onset

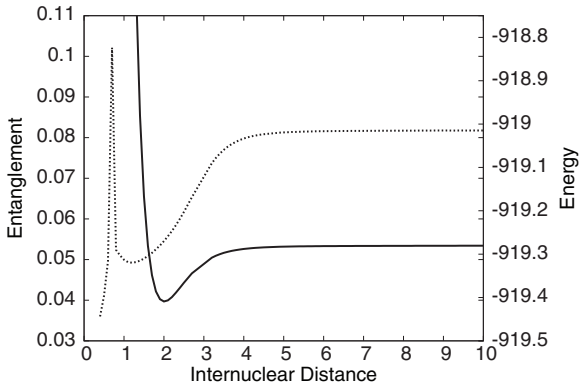

Figure 13. Entanglement (solid line) and total energy (dotted line) for the dissociation process of the chlorine molecule.

of the charge accumulation is observed from figure 15(b) and this is revealed by minima of both the entanglement and the atomic EP (see figure 14). At these points the atoms get their minimum capacity for acquiring electron charge, indicating a situation of electrostatic stability which anticipates the equilibrium situation marked by the minimum of the total

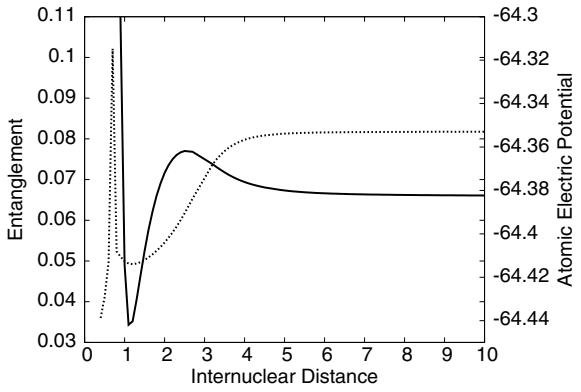

Figure 14. Entanglement (dotted line) and the atomic EP (solid line) for the dissociation process of the chlorine molecule.

energy shown at 2.0 Å (see figure 13) and also by the EP, which in this molecular case shows a maximum at this region, indicating a maximum capacity for the atoms to obtain more charge (see figure 14). This feature of the atomic EP reveals the higher electronegativity of these atoms as compared to the rest studied in this work. Continuing with the analysis, we find an interesting feature of the LAP at 1.9 Å which shows clearly (see figure 15(c)) a region of charge accumulation (non-nuclear maxima) at the equilibrium region. On the other hand, the MEP also reveals the equilibrium region through the forming of electrophilic regions enclosing the atoms, which starts the dissociation process and the bond cleavage (see figure 16(a)). At 3.5 Å the atoms are getting dissociated and this is indicated by all quantities which become constant at the onset of this region (see figures 13 and 14).

3.5. Hydrogen chloride molecule

The last system that we want to contemplate is the hydrogen chloride molecule. This example is of considerable interest because of its heteronuclear nature and also because of its polar bonding characteristics. This last feature implies a different type of dissociation process resulting in two clearly distinct atoms: the anionic chloride and the hydrogenic proton. It is thus interesting to verify whether the behaviour of the electronic entanglement is capable of revealing the structural changes exhibited by this system.

We proceed as in the previous cases. In figures 17 and 18, we have depicted the values for the entanglement measure (equation (1)) along with the total energy and the atomic EP (for both, hydrogen and chlorine), respectively. Interestingly, in the limiting cases, at $R \to 0$ and $R \to \infty$ the entanglement measure unveils the expected chemical situation, i.e. at the united-atom region the system behaves as the argon atom (see table 1) and at the dissociation region the molecular entropy tendency verifies the expected polar bonding for the chlorine anion at a very large extent (see table 2). Of course, this is a simple approach and it is likely that other states are mixed together so as to obtain the exact molecular value. Nevertheless, we think this is a fairly good approximation of the behaviour of the entanglement at large distances. Note from table 2 that the total energy for the molecular system coincides with twice the atomic ones for hydrogen and chlorine.

The behaviour of the physical quantities might be revealed by analysing the contours of the isosurfaces of the LAP and the MEP, which are shown in figures 19 and 20, respectively. First, it is interesting to appreciate from figure 19(a) that the LAP reveals the embedding of the hydrogenic atom into the most external shell of the chlorine atom and this point where hydrogen is extracted from the chlorine environment is marked by a shallow maximum of the entanglement measure (see figure 17). Next, as the bonding distance increases the atoms acquire different chemical features, due to the charge depletion of the hydrogen atom and the charge accumulation of the chlorine one. These changes, occurring when $R \approx 0.7$ Å, manifest themselves in the behaviour of both the entanglement and the energy. They correspond to a shallow minimum of entanglement and to the minimum of the EP for the chlorine atom (see figures 17 and 18). This behaviour reveals that the chlorine atom possesses its minimum capacity to acquire charge and this was already observed when the hydrogen atom separated from the chlorine environment (see figure 19(b)). Further, at 1.25 Å the system reaches its equilibrium configuration. This is indicated by the minimum of the total energy and by the minimum of the EP of the hydrogen atom (see figures 17 and 18). This is revealed by the LAP at this

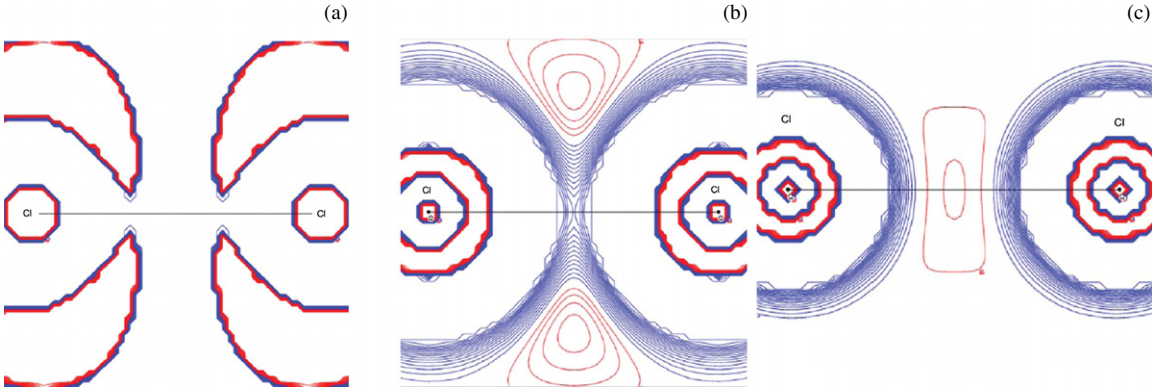

Figure 15. Contours of the isosurface of the LAP for the dissociation process of the chlorine molecule at an internuclear distance of 0.8 Å (left), 1.2 Å (center) and 1.9 Å (right).

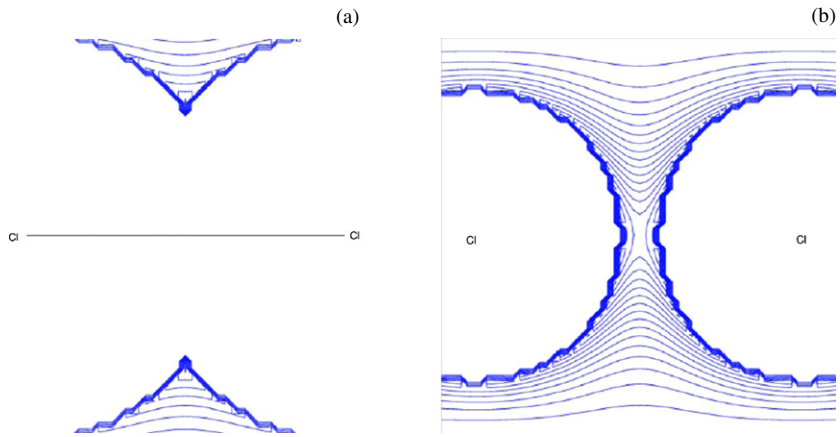

Figure 16. Contours of the isosurface of the MEP for the dissociation process of the chlorine molecule at an internuclear distance of 2.2 Å (left) and 3.0 Å (right).

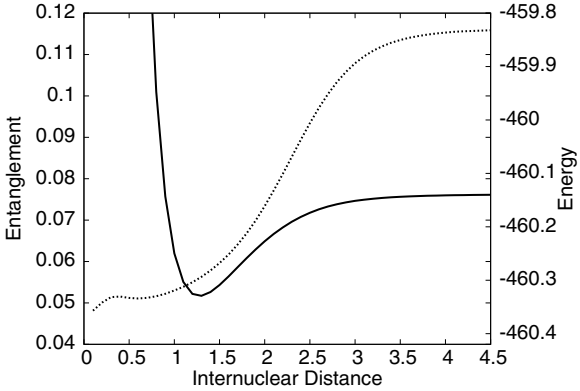

Figure 17. Entanglement (dotted line) and total energy (solid line) for the dissociation process of the hydrogen chloride molecule.

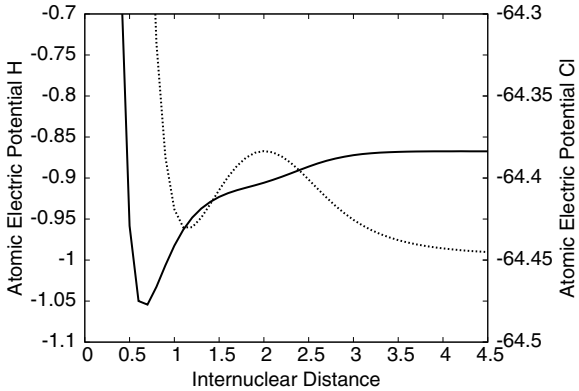

Figure 18. Atomic EP for chlorine (solid line) and hydrogen (dotted line) for the dissociation process of the hydrogen chloride molecule.

region, as it may be observed from figure 19(c) where the atoms became stabilized, i.e. the hydrogen atom possesses a low capacity to get negative density at the expense of the chlorine atom which shows an inflection point at this region (see figure 18). On the other hand, the MEP analysis reveals that at 2.0 Å the bond cleavage starts (see figure 20(a)) when the hydrogen atom gets its maximum capacity of acquiring charge at the expense of the chlorine atom which shows a shallow minima at this region. The onset of such a region marks the bonding features for this molecule as the atomic EP behave in opposite ways by increasing the acquired charge capacity of the chlorine atom at the expense of the hydrogen atom which shows a decreasing behaviour as it might be observed from figure 18. Finally, at 3.6 Å the MEP clearly indicates the ending of the molecular bond cleavage process. This is also revealed by the behaviour of other relevant physical quantities: electronic entanglement, energy and the atomic EP, all reaching at this stage an R-independent value.

According to the LAP analysis (charge depletion in red-coloured shades and charge accumulation in blue-coloured shades) that we have reported for each one of the molecules considered in this work, it is apparent that entanglement constitutes a highly sensitive quantity for detecting the built up of charge concentrations when the atoms approach each other. This fact is accentuated when one considers atoms with a larger number of electrons. As the number of electrons in the atoms participating in the molecular bonding process increases, the concomitant subshells tend to be more filled, and the lumping of electronic density becomes much more apparent. This is also linked with the electrophilic power (electronegativity) of these atoms, which depends on whether the valence shell is filled or not. These effects may explain an interesting feature shared by the dissociation processes of both the hydrogen and the hydrogen chloride molecules: neither of these cases exhibit a prominent peak for entanglement, when one considers the behaviour of this quantity as a function of the reaction coordinate R. This may be due to the fact that the participating hydrogenic atoms are endowed with just one single electron to 'share' when forming the bond and no extra charge is left, so no extra charge can be accumulated within the molecular bonding region. However, even in the case of the HCl molecule a very small peak can be detected when the atoms approach, due to the larger electronegativity for chlorine which embeds the hydrogen atom lumping a significant amount of charge in between the two. In contrast, at the other end, as the internuclear distance diminishes, the chlorine molecule shows a very pronounced peak for the entanglement measure due to the higher electronegativity holding for both atoms leading

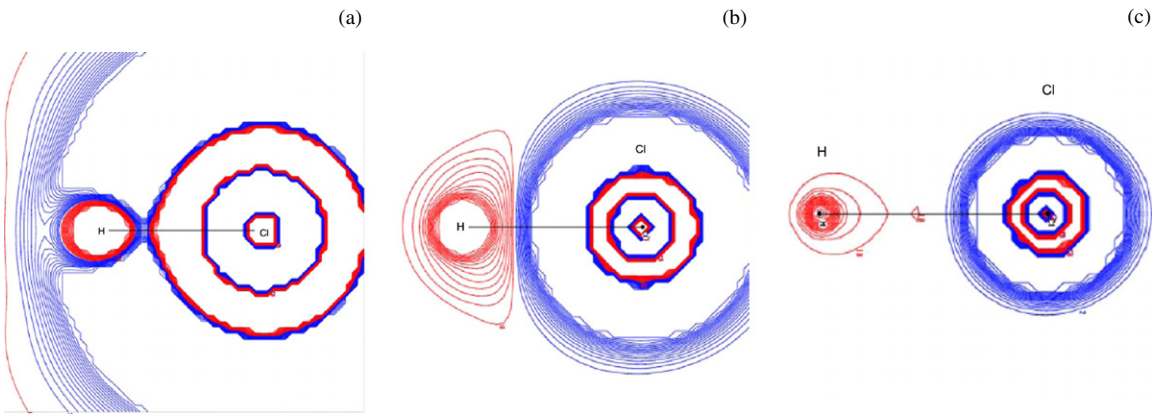

Figure 19. Contours of the isosurface of the LAP for the dissociation process of the hydrogen chloride molecule at an internuclear distance of 0.35 Å (left), 0.7 Å (center) and 1.25 Å (right).

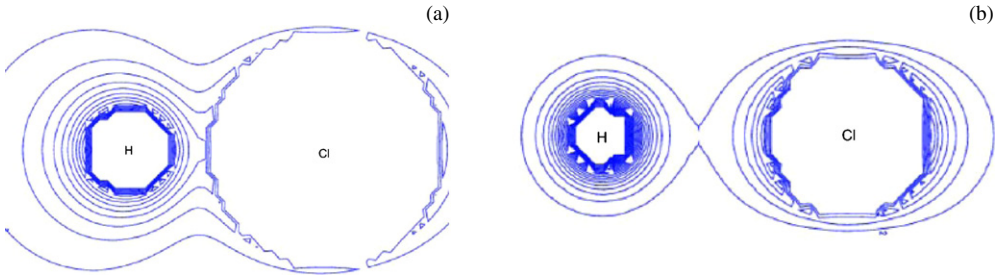

Figure 20. Contours of the isosurface of the MEP for the dissociation process of the hydrogen chloride molecule at an internuclear distance of 2.0 Å (left), and 3.6 Å (right).

to an increase of electron density and to the distortion of the valence shells of the atoms, as mentioned in section 3.4.

4. Conclusions

Throughout this work, we have performed an investigation of the electronic entanglement associated with homonuclear and heteronuclear diatomic molecules during a dissociation process. Analysing the isosurfaces of the LAP and the MEP our study revealed a number of remarkable correspondences between the evolution of the electronic entanglement as a function of the reaction coordinate R, on the one hand, and the main structural changes experienced by the molecular system during the dissociation process, on the other one. Indeed, the behaviour of the electronic entanglement as a function of R exhibits clear features that correspond to important changes in the chemically meaningful regions of the system. These features are observed for intermediate (finite) values of R. Regarding the limit cases $R \to 0$ and $R \to \infty$, the first one is given by the united-atom representation while the second one corresponds to the asymptotic limit when the atoms get dissociated. Indeed, as $R \to 0$ we observe that the amount of entanglement of the molecular system becomes small and approaches the entanglement of the united atom, consistently with the well-known fact that atomic eigenstates are described quite well by the Hartree–Fock approximation. On the other hand, the behaviour of the system's electronic entanglement in the limit $R \to \infty$ depends on the particular diatomic molecule considered, requiring thus a case by case analysis.

We think that this study may catalyze further work on the application of concepts from quantum information theory to the study of chemical systems and processes. In particular, it would be interesting to explore the entanglement features exhibited by more complex, polyatomic molecules. We expect to address this subject in a future communication.

Acknowledgments

ROE wishes to thank Juan Carlos Angulo and Jesús Sánchez-Dehesa for their kind hospitality during his sabbatical stay on the Departamento de Física Atómica, Molecular y Nuclear and the Instituto Carlos I de Física Teórica y Computacional at the Universidad de Granada, Spain. We acknowledge financial support through Mexican grants from CONACyT, PIFI, PROMEP-SEP and Spanish grants MICINN projects FIS-2008-02380, FQM-4643 and P06-FQM-2445 of the Junta de Andalucía. ROE wishes to acknowledge financial support from the Ministerio de Educación of Spain through grant SAB2009-0120 and also thanks Professor Marcelo Galván for his invaluable support and to E Martínez-Carrera for helpful discussions. Allocation of supercomputing time from the Laboratorio de Supercómputo y Visualización at UAM , the Sección de Supercomputacion at CSIRC-Universidad de Granada, and the Departamento de Supercómputo at DGSCA-UNAM is gratefully acknowledged.

References

[1] Amico L, Fazio L, Osterloh A and Vedral V 2008 *Rev. Mod. Phys.* **80** 517
[2] Tichy M C, Mintert F and Buchleitner A 2010 Essential entanglement for atomic and molecular physics arXiv:1012.3940v1
[3] Amovilli C and March N H 2004 *Phys. Rev.* A **69** 054302
[4] Carlier F, Mandilara A and Sarfati A 2007 *J. Phys. B: At. Mol. Opt. Phys.* **40** S199
[5] Osenda O and Serra P 2007 *Phys. Rev.* A **75** 042331
[6] Osenda O and Serra P 2008 *J. Phys. B: At. Mol. Opt. Phys.* **41** 065502
[7] Coe J P, Sudbery A and D'Amico I 2008 *Phys. Rev.* B **77** 205122
[8] Pipek J and Nagy I 2009 *Phys. Rev.* A **79** 052501
[9] Yañez R J, Plastino A R and Dehesa J S 2010 *Eur. Phys. J.* D **56** 141
[10] Manzano D, Plastino A R, Dehesa J S and Koga T 2010 *J. Phys. A: Math. Theor.* **43** 275301
[11] Aquilanti V, Bitencourt A C P, Ferreira C D S, Marzuoli A and Ragni M 2008 *Phys. Scr.* **78** 058103
[12] Nielsen M A and Chuang I L 2000 *Quantum Computation and Quantum Information* (Cambridge: Cambridge University Press)
[13] Lovett B W, Reina J H, Nazir A and Briggs A D 2003 *Phys. Rev.* B **68** 205319
[14] Liu J-L, Chen J-H and Voskoboynikov O 2006 *Comput. Phys. Commun.* **175** 575
[15] Bayer M 2011 *Nat. Phys.* **7** 103
[16] Cai J, Guerreschi G G and Briegel H J 2010 *Phys. Rev. Lett.* **104** 220502
[17] Cai J, Popescu S and Briegel H J 2010 *Phys. Rev.* E **82** 021921
[18] Arndt M, Juffmann T and Vedral V 2009 Quantum physics meets biology arXiv:0911.0155
[19] Wang H and Kais S 2007 *Isr. J. Chem.* **47** 5965
[20] Maiolo T A C, Della Sala F, Martina L and Soliani G 2007 *Theor. Math. Phys.* **152** 1146
[21] Das C and Bhattacharyya K 2009 *Phys. Rev.* A **79** 012107
[22] Gonzalez-Ferez R and Dehesa J S 2003 *Phys. Rev. Lett.* **91** 113001
[23] Dehesa J S, Gonzalez-Ferez R and Sanchez-Moreno P 2007 *J. Phys. A: Math. Theor.* **40** 1845
[24] Liu S 2007 *J. Chem. Phys.* **126** 191107
[25] Nagy A 2007 *Chem. Phys. Lett.* **449** 212
[26] Nagy A 2006 *Chem. Phys. Lett.* **425** 154
[27] Glasser M L and Nieto L M 2005 *J. Phys. A: Math. Gen.* **38** L455
[28] Plastino A R and Plastino A 1993 *Phys. Lett.* A **181** 446
[29] Esquivel R O, Flores-Gallegos N, Iuga C, Carrera E, Angulo J C and Antolin J 2009 *Theor. Chem. Acc.* **124** 445
[30] Eckert K, Schliemann J, Bruss D and Lewenstein M 2002 *Ann. Phys.* **299** 88
[31] Ghirardi G, Marinatto L and Weber T 2002 *J. Stat. Phys.* **108** 49
[32] Ghirardi G and Marinatto L 2004 *Phys. Rev.* A **70** 012109
[33] Naudts J and Verhulst T 2007 *Phys. Rev.* A **75** 062104
[34] Borras A, Plastino A R, Casas M and Plastino A 2008 *Phys. Rev.* A **78** 052104
[35] Zander C and Plastino A R 2010 *Phys. Rev.* A **81** 062128
[36] Oliveira V C G, Santos H A B, Torres L A M and Souza A M C 2008 *Int. J. Quantum Inf.* **6** 379
[37] Plastino A R, Manzano D and Dehesa J S 2009 *Europhys. Lett.* **86** 20005
[38] Löwdin P O 1970 *Adv. Quantum Chem.* **5** 185
Löwdin P O 1955 *Phys. Rev.* **97** 1474
Löwdin P O and Shull H 1956 *Phys. Rev.* **101** 1730
[39] Flores-Gallegos N and Esquivel R O 2008 *J. Mex. Chem. Soc.* **52** 19
[40] Carrera E, Flores-Gallegos N and Esquivel R O 2010 *J. Comput. Appl. Math.* **233** 1483
[41] Bader R F W 1994 *Atoms in Molecules* (New York: Oxford University Press)
[42] Politzer P and Truhlar D G 1981 *Chemical Applications of Atomic and Molecular Electrostatic Potentials* (New York: Academic)
[43] Francl M M, Pietro W J, Henre W J, Binkley J S, Gordon M S, DeFrees D J and Pople J A 1982 *J. Chem. Phys.* **77** 3654
[44] Dunning T H 1989 *J. Chem. Phys.* **90** 1007
[45] Frisch M J *et al* 2004 *GAUSSIAN03*, Revision D.01 (Wallingford CT: Gaussian Inc.)
[46] Schaftenaar G and Noordik J H 2000 MOLDEN: a pre- and post-processing program for molecular and electronic structures *J. Computeraided Mol. Des.* **14** 123
[47] Breneman M and Wiberg K B 1990 *J. Comput. Chem.* **11** 361
[48] Birks J B 1975 *Rep. Prog. Phys.* **38** 903
[49] Kurunczia P, Lopeza J, Shaha H and Becker K 2001 *Int. J. Mass Spectrom.* **205** 277
[50] Edgecombe K E, Esquivel R O, Smith V H Jr and Müller-Plathe F 1992 *J. Chem. Phys.* **97** 2593
[51] Madsen G K H, Blaha P and Schwarz K 2002 *J. Chem. Phys.* **117** 8030
[52] Cioslowski J 1990 *J. Phys. Chem.* **94** 5496
see also Cooper D 1990 *Nature* **346** 796